Title: Macrophage chemotaxis steered by complex self-generated gradients of complement C5a

Authors:

Abhimanyu Kiran[a,b], Peter A. Thomason[a], David M. Versluis[b], Peggy I. Paschke[a], Hannah Donnelly[a†] , Luke Tweedy[a], Sergio Lilla[a], Isabel Bravo-Ferrer[b], Amy Shergold[a], Ryan Devlin[a], Ed W. Roberts[a], Robert H. Insall [a,b,*]

Affiliations:

[a] CRUK Scotland Institute, Bearsden, Glasgow G61 1BD, UK

[b] Division of Cell & Developmental Biology, University College London, London WC1E 6BT, UK

*Corresponding author. Email: R.Insall@ucl.ac.uk.

†Current address: School of Molecular Biosciences, University of Glasgow, Glasgow G12 8QQ, UK

Abstract:

Macrophages rely on efficient chemotaxis to locate sites of infection and tissue damage. One general strategy that enhances chemotactic accuracy is the use of self-generated gradients, where cells locally deplete attractants to create or sharpen guidance cues. Here we show that mouse bone marrow–derived macrophages (BMDMs) migrate toward the complement component C5a using this strategy. Cells actively deplete C5a from their surroundings, establishing local gradients as fresh attractant diffuses inward. We visualized this process in real time with fluorescent C5a and reproduced its dynamics using computational models. C5a depletion is mediated primarily by C5aR1-dependent endocytosis. This mechanism produces complex responses, with different C5a concentrations inducing temporally distinct waves of migration, and maximal chemotaxis occurring below 10 nM C5a. As expected, increasing C5a concentrations recruit more cells. In contrast, human macrophages inactivate C5a mainly through carboxypeptidase-mediated enzymatic degradation, yielding a higher optimal concentration (~30 nM) and distinct migratory dynamics. Both species also deplete externally imposed C5a gradients, sharpening them and enhancing guidance.

These findings identify C5a degradation as a critical mechanism by which macrophages extract directional information from their environment. Self-generated gradient formation, despite different mechanisms across species, emerges as a conserved and versatile strategy for immune navigation.

INTRODUCTION

Cell migration is a fundamental biological process involved in embryo implantation, development, cancer metastasis, wound healing, and immune cell function (1, 2). While cells can migrate randomly, it is extremely inefficient over most physiological scales; efficient migration in vivo is usually guided by directional cues from the environment. Among the best-understood guidance cues are diffusible chemicals—chemoattractants—which form gradients interpreted by receptors on the cell surface. The direction and steepness of the gradients provide steering cues that are interpreted through receptors, most often seven transmembrane receptors that couple to G proteins, yielding chemotaxis - cell migration directed towards the source of the chemoattractant (3, 4).

For immune cells, chemoattractants fall into two main categories: those produced by the target (e.g., formyl peptides like fMLP from bacteria) and those produced by the host, such as chemokines or complement-derived peptides like C5a (5, 6). Immune cells detect these gradients and efficiently migrate toward their sources (7-9).

Macrophages are a critical immune cell population, essential to the body's defence system, that respond rapidly to infections. They perform diverse functions including pathogen engulfment (phagocytosis), antigen presentation, and tissue repair. Macrophages can arise from circulating monocytes that infiltrate tissues, or from long-lived tissue-resident populations established during early development (10, 11).

Within tissues, macrophages constantly sample their environment using pattern recognition receptors (PRRs) to detect pathogen-associated molecular patterns. Once activated, they migrate directionally toward infection sites, guided by chemokines from other immune cells and complement factors such as C5a and C3a (12, 13). C5a is one of the most potent chemoattractants known, for macrophages and also neutrophils. It is produced at sites of complement activation, a clear hallmark of tissue damage, by proteolysis from the much larger C5 molecule.

However, the gradients of these chemical signals at infection sites are not always well-defined. Attractants are often initially uniform, or spread into shallow gradients by tissues. Consequently, to navigate effectively, cells must locally modify or degrade these constant concentrations to create steep gradients, facilitating their precise migration towards the source of

infection. This phenomenon, known as self-generated chemotaxis, has been observed in various cell types, including various cancers, dendritic cells, and model organisms such as zebrafish and Dictyostelium (14-18).

Although C5a is known as a dominant chemoattractant for macrophages, it is unclear how macrophages navigate when C5a is abundant but not spatially structured. We therefore asked whether they, like other systems, could generate their own navigational cues. C5a biology makes it an especially suitable context to test self-generated guidance. It is generated rapidly and diffusely during complement activation (5), often creating high but poorly directional concentrations (19). Macrophages express high levels of its receptor, C5AR1. At the same time, its activity is curtailed by multiple macrophage-expressed mechanisms, including endocytosis, degradation, and enzymatic trimming. These features suggest that macrophages are not merely passive responders but may actively remodel C5a fields to create navigational cues.

We now demonstrate that mouse bone marrow-derived macrophages (BMDMs) employ self-generated gradients to steer toward C5a. The cells endocytose or degrade the C5a ligand while they respond to it, creating gradients even in initially uniform environments and sharpening pre-existing gradients around the responders. This represents, to our knowledge, the first demonstration of self-generated chemotaxis in macrophages, and fills a missing piece in our picture of host defence.

RESULTS

Macrophages create and migrate up chemotactic gradients of C5a

Complement C5a is among the most potent chemoattractants for macrophages (20). In most experimental setups, it is presented to cells as a premade linear gradient, typically formed between two reservoirs, one containing no C5a and the other a substantial concentration. However, our research on cells including different cancer types and *Dictyostelium*, backed up by computational models, has shown that cells can chemotax more efficiently to gradients formed locally by the responding cells themselves (21-23). We therefore tested the ability of bone marrow derived macrophages (BMDMs) to self-generate gradients of C5a and navigate using them.

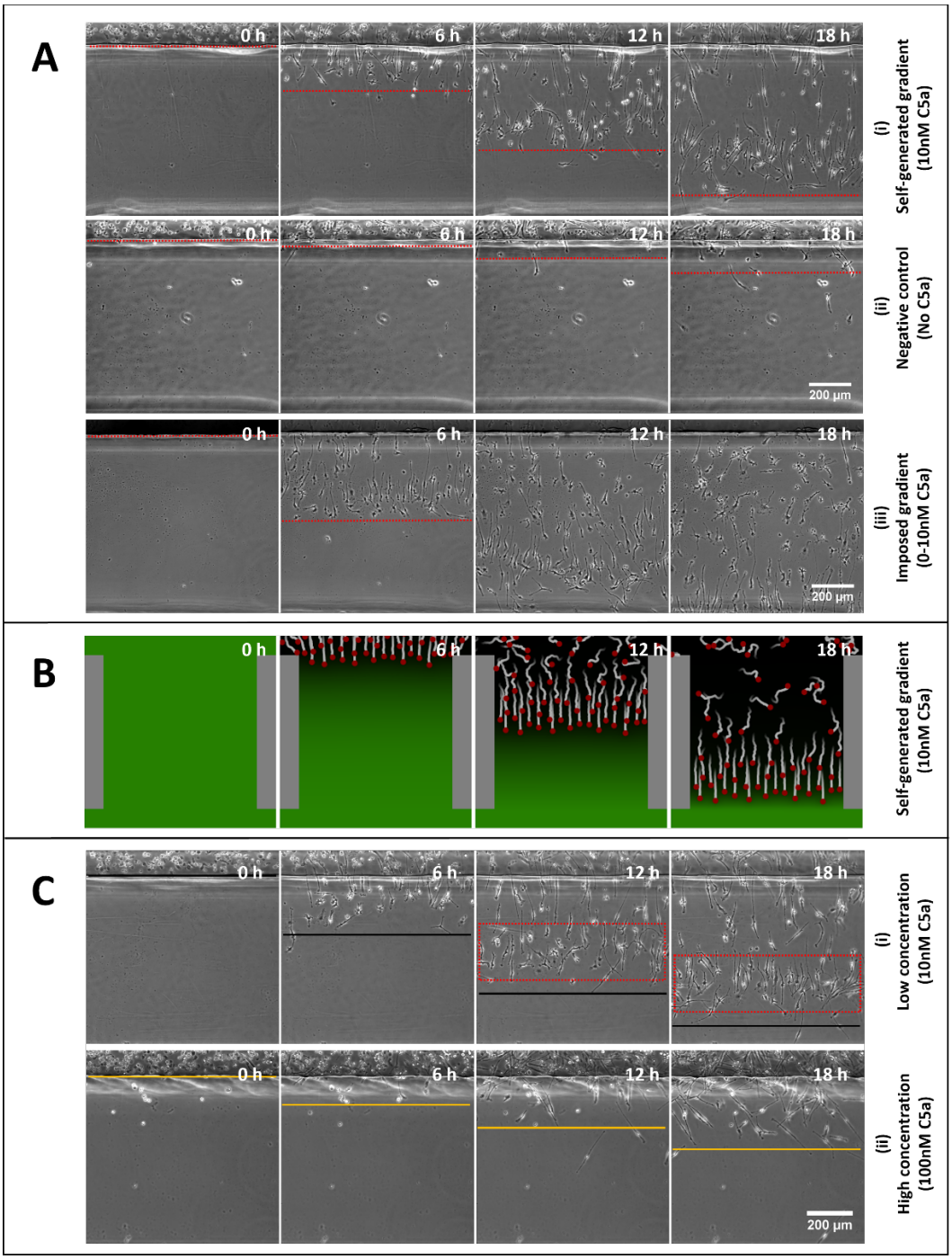

Figure 1: Self-generated chemotaxis of mouse macrophages to C5a.
(A) BMDM responses to (i) an initially homogeneous concentration of 10 nM C5a, (ii) negative control (no C5a), and (iii) an imposed gradient of 0–10 nM C5a.
(B) Computational simulation, using parameters from experimental data, showing cells depleting C5a from a homogeneous 10 nM environment and migrating up the resulting self-generated gradient.
(C) Self-generated gradient responses at (i) 10 nM C5a and (ii) 100 nM C5a. Red dashed box highlights the leading cell wave. Solid black and yellow lines indicate the distance covered by cells on the bridge at low and high concentrations, respectively.

We filled an Insall chemotaxis chamber (24) with a homogeneous concentration of 10nM C5a (that is, initially 10nM C5a in both wells and the bridge between) and introduced 1.5×10^6 BMDMs/ml to the outer well. If the cells efficiently depleted the C5a present in the outer well, a chemotactic gradient would be established along the bridge; if they did not, the cells would migrate randomly without steering cues, and mostly remain in the well. Figure 1A and movie S1 show efficient self-generated chemotaxis of remarkable efficiency – despite initially homogeneous C5a, macrophages oriented accurately towards the opposite well and migrated directly away from their initial reservoir. The negative control showed almost no migration over this timescale (Figure 1A and movie S1), confirming that the migration depends on the presence of C5a. Thus, macrophages are able to self-generate C5a gradients and simultaneously respond to them.

Inspired by the experimental observations, a hybrid agent-based computational simulation was performed, based on earlier modelling work by our lab (16) and using parameters derived from measurements, listed in Supplementary Table 1. In these simulations, each cell independently degrades the chemoattractant in its immediate vicinity and moves up gradients of attractant. When initialised with a uniform concentration of chemoattractant, simulations were able to replicate the experimental observations (Fig. 1B and Movie S2), indicating that locally degrading attractant can lead to an effective self-generated gradient, and effectively illustrating the mechanism underlying the chemotaxis.

One defining feature of self-generated chemotactic gradients is a collective wave at the front of the population of migrating cells (25). Macrophages migrating in C5a show a particularly clear front wave (Figure 1A, compare (i) and (iii) at 18h; red box in Figure 1C). These cells are particularly accurately aligned towards the opposite well, and migrate as a coherent group. Another behaviour particularly noted in self-generated chemotaxis is that high attractant concentrations cause a delay before the wave of chemotaxis begins (the time it takes for the cells to clear the attractant out of their well) and slower directional migration of the cells in the wave (25). We analysed the response of macrophages to a substantially higher concentration of C5a (100nM). Figure 1C and Movie S3 show that the cells took significantly longer to start chemotaxing and enter the bridge than at 10nM, though still obviously better than the negative control. Interestingly,

the alignment of the cells in the front wave was strikingly different in both the cases. With 10nM C5a the cells in the front wave were inclined to ~90° to the bridge (Figure 1C); with 100nM the alignment was nearer ~45°, implying a much less legible gradient, presumably because cells struggled to clear the C5a from their rears, or because persistent migration carried them into regions of C5a saturation.

It is also clear that the positive control with a simple 0-10nM gradient (Figure 1A, Movie S4) shows a wave of particularly well-oriented cells at the front, with decreased chemotaxis behind. This behaviour is not expected from cells responding simply to an imposed gradient. This implies that the same mechanisms that create self-generated gradients also act to shape imposed gradients, as has been seen for example in melanoma chemotaxis (21).

Effects of Lipopolysaccharide Activation

Activation in the presence of bacterial or pathogen traces is a fundamental feature of macrophage biology. We therefore examined self-generated chemotaxis in LPS- activated and inactivated macrophages. The LPS binds and activates the Toll-like receptor 4 (TLR4) on the surface of the macrophage, triggering a signalling cascade that alters gene expression and leads to the production of inflammatory cytokines and mediators (26).

LPS stimulation was not essential for self-generated chemotaxis. Both activated and inactivated macrophages respond effectively to homogeneous C5a, and start to migrate at the same time. However, the inactivated macrophages chemotax less accurately than LPS-activated ones. Clearly, both activated and inactivated macrophages express a high enough level of C5a receptors to steer. The differences therefore more likely reflect changes in the pathways that connect gradients to migration and steering, or proinflammatory responses after activation.

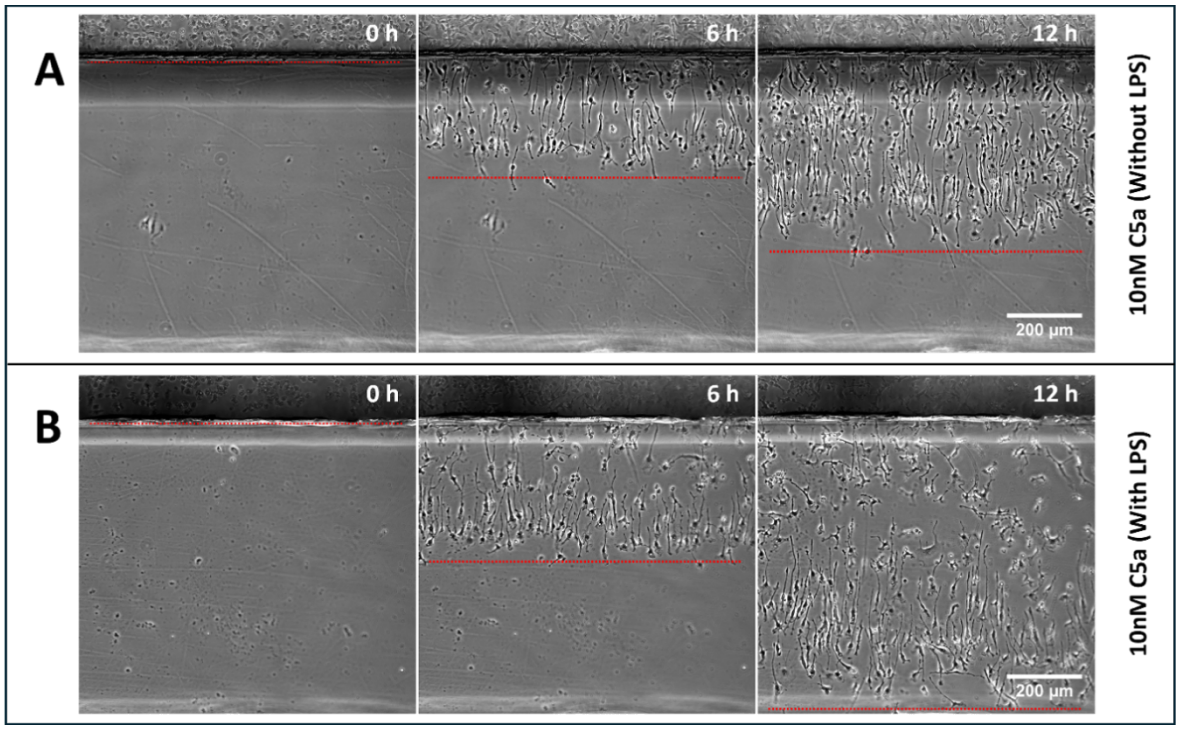

Figure 2: LPS stimulation of self-generated chemotaxis of BMDMs to C5a.

BMDM migration in response to homogeneous C5a in the absence (A) or presence (B) of lipopolysaccharide (LPS) stimulation. In both conditions, cells established self-generated gradients and migrated across the bridge, but LPS-activated macrophages showed greater accuracy and coherence in their directional movement. Red dashed lines outline the regions occupied by migrating cells on the bridge.

Dose Dependence of Self-Generated C5a Chemotaxis

In other cell types, we have shown that the number of cells in the front wave of a self-generated gradient is approximately proportional to the attractant concentration (16, 23). We tested whether this holds for BMDMs using self-generated gradients formed from initial C5a concentrations of 0.3nM, 3nM & 30nM (Movie S5). Figure 3A shows responses of the same initial cell density after 6h. As expected, few cells entered the bridge at 0.3nM C5a, because that is all that is required to inactivate or remove all of the C5a as it diffuses from the source well. With 3nM C5a, the number of cells in the front wave was clearly greater (Figure 3A(ii)), but only by about twofold despite the 10x increase in chemoattractant. The same was true at the yet higher concentration of 30nM C5a; after an initial delay for the cells to deplete the pool (see above), a larger wave still was formed (Figure 3A(iii)), but again with less than threefold further increase in cell number despite a 10x

increase in attractant. Again, negative controls with no C5a gave negligible migration under these conditions (Figure 3B). Note also the slower response at higher concentrations as described earlier. We would expect an approximately linear relationship between attractant concentration and the number of cells in the wave. The actual result suggests an extra level of complexity. One possibility is that cells are increasing their rate of breakdown at higher C5a concentrations, for example, proposed induction of extra breakdown enzymes at high ligand occupancy as a mechanism to increase robustness (23). Another is that cells are communicating with one another through additional mechanisms than simple C5a depletion.

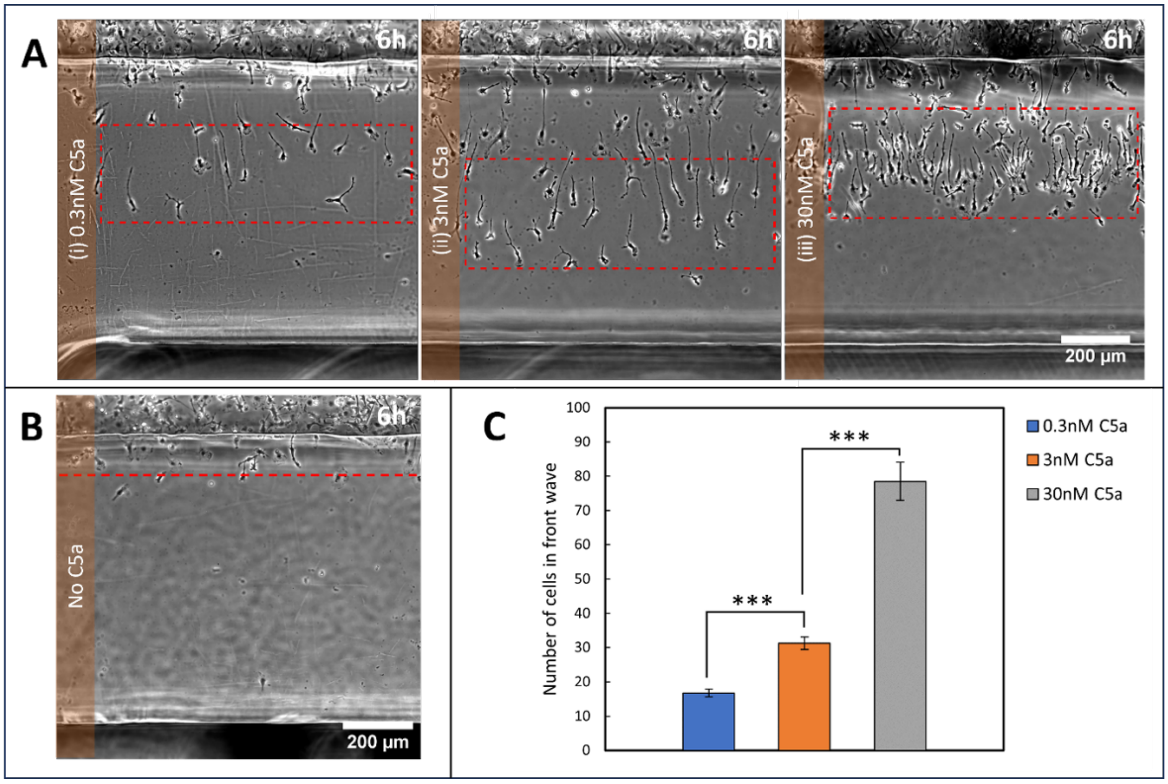

Figure 3. Dose dependence of self-generated chemotaxis to C5a.
(A) Representative images showing BMDM migration after 6 h in initially homogeneous C5a concentrations of (i) 0.3 nM, (ii) 3 nM, and (iii) 30 nM. Red dashed boxes highlight the front wave of cells.
(B) Negative control (no C5a), showing negligible migration. Red dashed line indicates the region assessed for cell migration.
(C) Quantification of cells in the front wave at different C5a concentrations after 6 h. Data are shown as mean ± SD. Statistical significance was assessed using Student's *t*-test; *** indicates $p < 0.0001$.

BMDMs deplete C5a from their surroundings using endocytosis

To perform self-generated chemotaxis, macrophages must get rid of the C5a in their local environment to form locally steep gradients. Two general mechanisms for this have been described – first, using enzymes that convert the chemoattractant into an inactive form (21, 27), and second, by receptor-mediated endocytosis of the chemoattractant (14, 28). The enzymes may be membrane-bound with their catalytic domains exposed to the extracellular medium, like LPP3, or secreted, like phosphodiesterases. One strong candidate enzyme, carboxypeptidase M, is known to inactivate C5a in a complicated fashion by trimming off the C-terminal arginine (29), and is specifically expressed in human macrophages. However, mouse macrophages such as our BMDMs do not express carboxypeptidase M (see, for example, the Immunological Genome Project - https://rstats.immgen.org/Skyline/skyline.html). We also examined C5a by mass spectrometry after incubation with BMDMs. The trimmed C5a (C5a-des-R) was not detected when mouse cells were incubated with C5a, whereas it was detected in all samples where THP-1 cultured human macrophages were used (Supplementary figure 1). Interestingly, a hitherto undescribed double-trimmed form (C5a-des-GR) was also seen in the human and not mouse experiments. Mouse macrophages express a range of other secreted and membrane-bound proteases, but CPM is the only enzyme known to degrade C5a.

To further distinguish endocytic from enzymatic degradation, we used commercially available C5a labelled with fluorescent AF647 at its N-terminus. Extracellular enzymes such as proteases do not change the fluorescence of this molecule when they attack it – trimming the C5a into an inactive form does not alter its fluorescence, so active and inactive molecules fluoresce the same. However, endocytosis should be visible as a loss of fluorescence from the medium and a sharp gain in vesicles inside the cell (30). We visualized both medium and intracellular detail in BMDMs migrating up a self-generated AF647-C5a gradient, examining both using a confocal microscope, after the cells had moved some distance across the bridge. The results are striking (Figure 4) – BMDMs internalize the labelled C5a, and remove it from the medium, creating a gradient. The chambers, which were set up with homogenous C5a, show a clear gradient after a few hours' incubation with cells – low in the immediate vicinity of the BMDMs, becoming higher by 200µm away. Soon after the chamber has been assembled, the macrophages contain punctate fluorescence, reflecting the endocytosed C5a and its breakdown products.

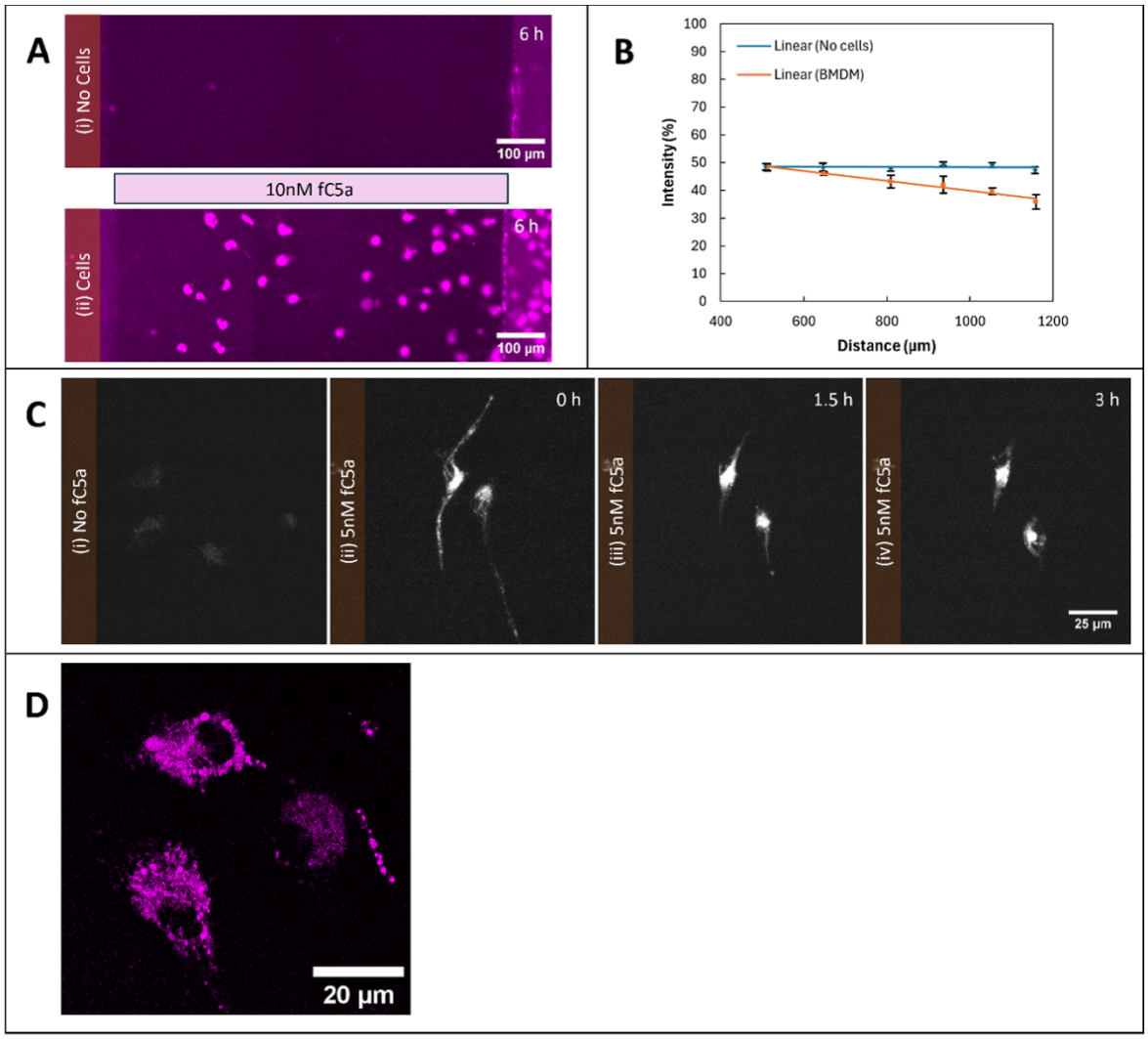

Figure 4. Receptor-mediated uptake of C5a by BMDMs.
(A) Distribution of fluorescent AF647-C5a after incubation without (i) or with (ii) BMDMs.
(B) Quantification of fluorescence intensity along the bridge in the presence or absence of BMDMs, showing depletion of C5a near the cells.
(C) Time course of C5a uptake. BMDMs were exposed to 5 nM AF647-C5a for 1 h, washed, and imaged at 0, 1.5, and 3 h. Fluorescence localized to intracellular puncta and accumulated near the perinuclear region, consistent with endocytosis and lysosomal processing. Images were captured and processed using identical acquisition parameters.
(D) Magnified view showing AF647-C5a in vesicular structures 1.5h after exposure. Cells prepared as in C.

Thus, BMDMs set up their own chemoattractant gradients by endocytosing C5a from their surroundings, and retaining it, presumably for lysosomal breakdown.

234 Endocytosed C5a could be recycled and re-secreted or targeted to lysosomes and broken down. To
235 explore this mechanism, cells were seeded in Petri dishes at a similar density to the chemotaxis
236 chambers, exposed to 5nM of C5a-AF647 for 1 hour, then washed with fresh medium and
237 examined after different intervals (Figure 4C (i-iv)). This clearly shows the cells retain the C5a
238 they take up. The fluorescent signal appeared to be in endocytic vesicles and eventually localized
239 in the perinuclear region (Figure 4C), and was not released in significant quantities over three
240 hours.
241

242 **Comparison between human and mouse macrophages**

243 We hypothesized that the presence of CPM in human macrophages might alter the way they made
244 and responded to self-generated gradients. Human macrophages could use the surface bound
245 enzyme to get rid of C5a in their local environment, in contrast to the receptor mediated
246 endocytosis employed by the mouse macrophages. We tested this hypothesis several ways. First,
247 we observed the change in the extracellular imposed gradient of fluorescent AF647-C5a by the
248 macrophages over time. Interestingly, although both types of macrophage could perform self-
249 generated chemotaxis, only the mouse cells were able to affect the fluorescence profile of the C5a
250 gradient (Figure 5A-B), demonstrating a role of receptor mediated endocytosis in depleting C5a
251 from the environment. For human macrophages (Figure 5C-D), the gradient of fluorescence
252 remained similar, suggesting that the C5a was mainly being inactivated by the surface bound
253 enzyme rather than endocytosed.

254 The different mechanism of establishing self-generated gradients would be expected to lead to
255 different behaviours. In particular, the K_d of receptors is typically much lower than the K_m of
256 enzymes, so receptor-mediated mechanisms typically work at a lower ligand concentration than
257 enzyme-mediated ones. The dose response of both types of macrophages was assessed by counting
258 the number of cells crossing a line 200μm along the bridge after 18 hours for various C5a
259 concentrations. As predicted, the human cells steered most effectively at a higher C5a
260 concentration (>30nM vs 10nM, Figure 5E). Tracking the chemotaxis of both types of
261 macrophage, using 3nM C5a so as to be below the saturation for both types of macrophage (Figure
262 5F), showed that human macrophages performed much better at the higher end of the gradient.
263 This presumably reflects their greater ability to degrade the chemoattractant in their vicinity,
264 forming steeper and more robust gradients compared to mouse macrophages, which can only

internalize one C5a molecule at a time through receptor endocytosis and are thus limited by receptor availability at the cell surface.

The collective behaviour is also different - mouse macrophages show synchronized motion among themselves to form a clearly visible front wave (Figure 3A), whereas the human macrophages chemotax more independently (Movie S6). Interestingly, the human macrophages can operate within a broader range of chemoattractant concentrations (Figure 5E), showing a clear response at very low concentrations as well as a better one at higher concentrations. This robustness is a predicted outcome of systems that use chemoattractant-degrading enzymes as well as receptor-mediated uptake (16, 23).

Mouse and human macrophages behaved dissimilarly when performing self-generated chemotaxis to 3nM of C5a. Although they had a very similar time independent chemotaxis index ($\cos\theta$ – see Figure 5G), the average speed of the human macrophages was twice as that of mouse macrophages (Figure 5H). The speed of the chemotactic wave depends predominantly on the interaction between the Vmax of C5a degradation and its diffusion, rather than the inherent speed of the cells, so fast migration of human cells is consistent with rapid degradation of C5a, again consistent with the involvement of surface bound enzymes.

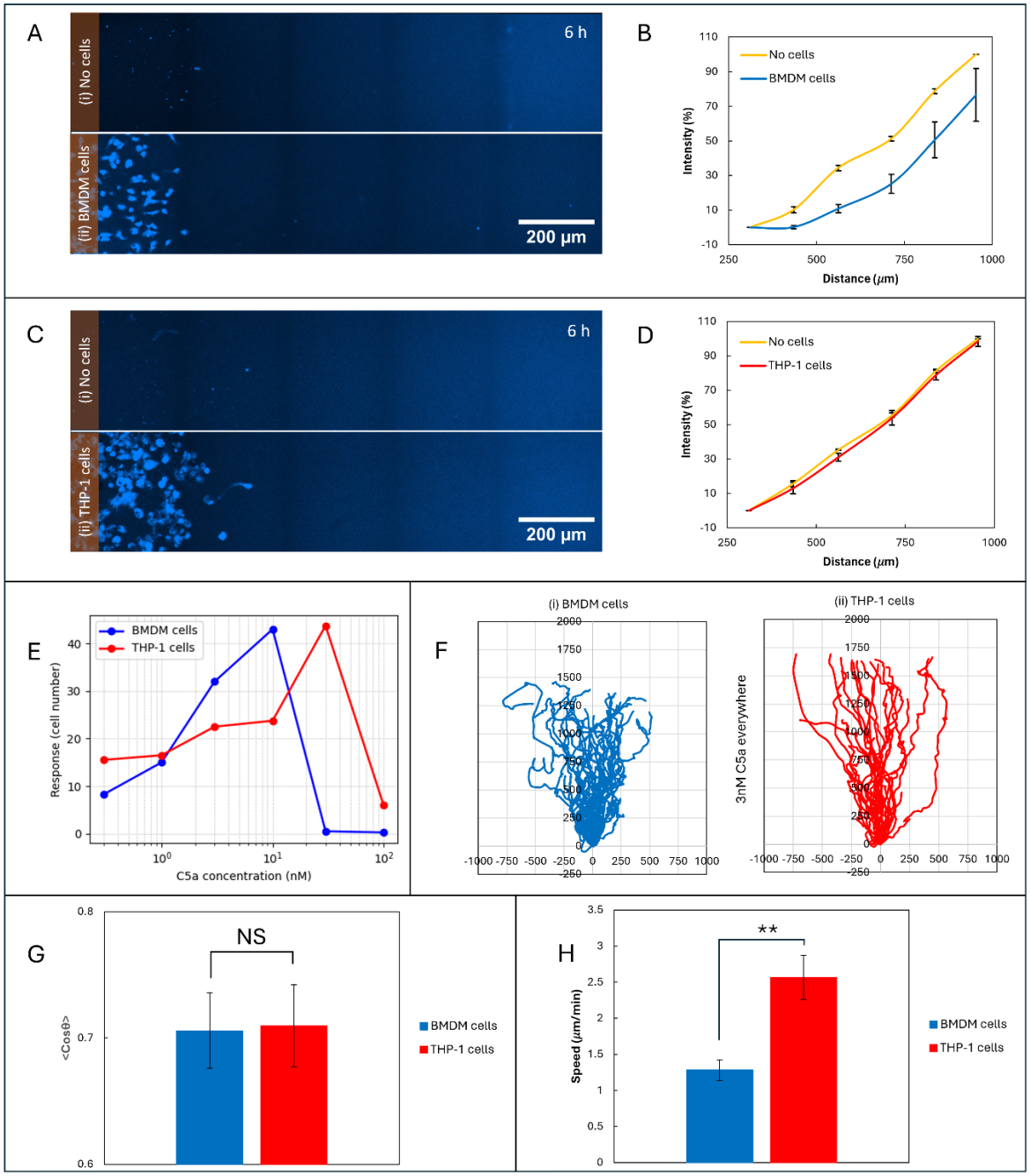

Fig 5: Different C5a inactivation mechanisms in mouse and human macrophages. A. A gradient of fluorescent C5a was established in an Insall chamber with & without mouse BMDM cells. B. measurement of fluorescent intensity along the bridge with and without BMDM cells, C. Imposed gradient of fluorescent C5a (i) without, & with THP-1 cells, & D. Measured intensity along the bridge with & without THP-1 cells, E. Dose response of chemotaxis. The number of cells that had migrated 200μm along the bridge was measured after 18hr for different C5a concentrations. G, H: Comparing the self-generated chemotaxis of mouse & human macrophages to 3nM C5a showed insignificant difference in their cosθ (G), but significant difference in the mean speed (H). Bar in G and H = SE (n=4). ** represents p-value < 0.001.

293 **C5aR1 mediates C5a chemotaxis**

294

295 C5a is transduced by two cell-surface receptors, C5aR1 and C5aR2. Most authors consider C5aR1
296 to be the primary chemotactic receptor (31).
297 C5aR2's role is less clear. It may transduce a subset of signals, or may be a scavenger receptor,
298 in which case it could play a role in the formation of self-generated gradients. To test whether
299 C5aR1 or C5aR2 was forming the gradient, we employed a non-competitive receptor antagonist
300 PMX-53 which inhibits the binding of C5a to C5aR1 but does not affect binding to C5aR2. We
301 verified the inhibitor was effective by imaging macrophages chemotaxing up an imposed gradient
302 of 0-10nM C5a in the presence or absence of 10uM PMX-53 (Figure 6A&B, Movie S7). The
303 inhibitor is clearly effective - the untreated cells show longer and better-directed trajectories
304 (Figure 6A,C) than inhibited ones (Figure 6B,D). The average speed of the cells with positive
305 control and inhibitor control was 1.25μm/min and 1.06μm/min, respectively, implying that the
306 inhibitor does not affect the cell's underlying ability to migrate, but mean cosθ dropped from 0.4
307 to 0.2 after inhibitor treatment (Fig. 6E). Thus as expected C5aR1 is the receptor that mediates
308 chemotaxis.
309 Imaging receptor-mediated uptake of AF647-C5a in the presence and absence of PMX-53
310 demonstrated that C5aR1 was also the receptor mediating C5a uptake. Cells were seeded in 8-well
311 glass bottom dishes, with or without pretreatment with 10μM PMX-53 for 30 min. After this,
312 10nM AF647-C5a was added and incubated for 1 hour, before assessing C5a uptake using a
313 confocal microscope. As previously, untreated macrophages contained high levels of C5a, but
314 inhibitor-treated cells showed strikingly less (Figure 6F, quantified in Figure 6G) – the total
315 fluorescence endocytosed in the cells dropped by >60%. As receptor inhibitors are not completely
316 efficient, this implies that an even greater fraction of the C5a uptake from the environment was
317 mediated by C5aR1.
318

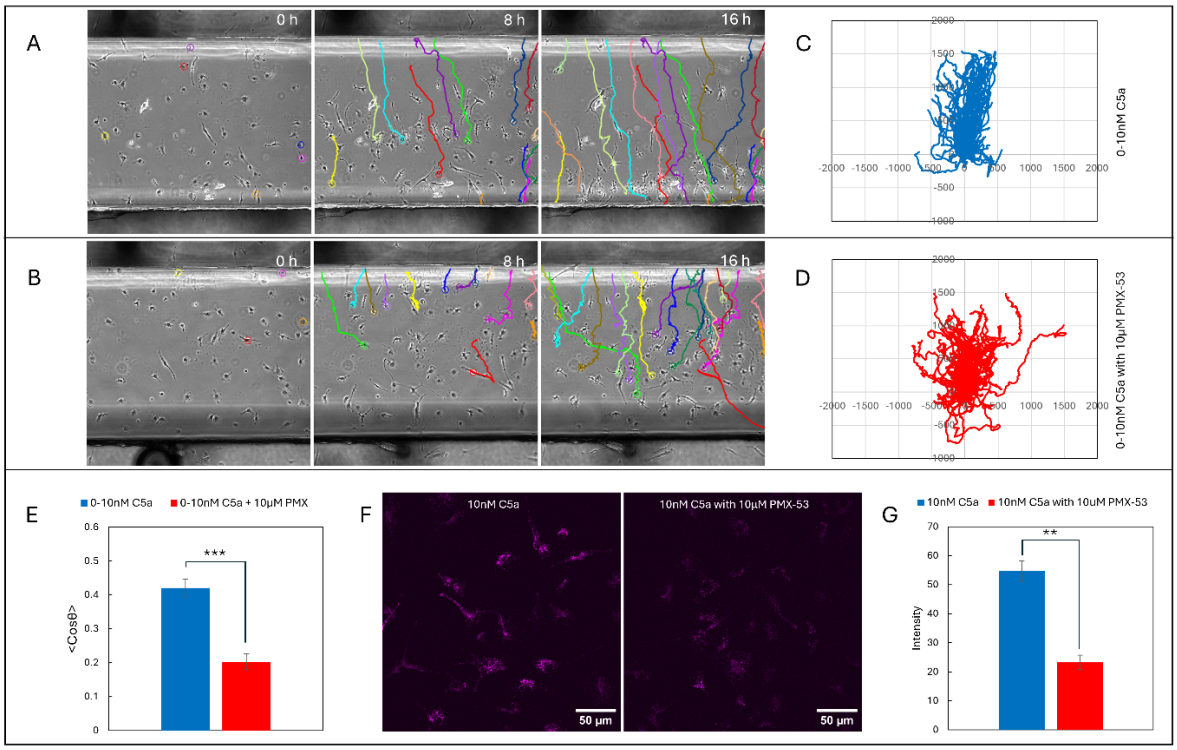

Fig 6: Receptor mediated C5a uptake via C5aR1. Time-lapse images of cells subjected to A. 0-10nM C5a with cells tracks, B. 0-10nM C5a in the presence of 10uM PMX-53 (inhibitor), C. Spider plot for the 0-10nM C5a, D. Spider plot for the 0-10nM C5a in the presence of 10uM PMX-53, E. Comparison of chemotaxis index for both the cases with and without inhibitor, F. Confocal images indicating the C5a AF647® uptake and G. quantification of cellular intensity (bars show mean± SEM, n=3; ** student's t-test p-value <0.001)

DISCUSSION

Anaphylatoxin C5a, a small peptide released as a result of complement activation, is a strong chemoattractant for macrophages (32). Studies over many years and using widely different methods have shown mouse bone marrow-derived (33-35) and other (36, 37) macrophages perform efficient chemotaxis up gradients of a range of attractants (33) including C5a (38, 39). Here we have shown, for the first time, that macrophages can perform self-generated gradient (SGG) chemotaxis towards C5a, turning a flat concentration of C5a into a gradient, then migrating up it (Figure 1A(i)). Self-generated gradients are an efficient and often counterintuitive way for cells to probe their environment and obtain dynamic and complex information about the best paths (40-42); this mode of steering is feasible and believed to occur frequently in real biological scenarios.

For efficient chemotaxis, the cells need to deplete the chemoattractant available in their immediate vicinity at a rate that is sufficient to overcome new production and diffusion from the environment. Two well-established mechanisms by which cells can degrade chemoattractants have been found to set up self-generated gradients. The first uses surface-bound enzymes, with their active sites on the extracellular side, that degrade and inactivate the local chemoattractant. When we first observed a front wave in macrophage chemotaxis, suggesting a self-generated gradient, membrane-bound carboxypeptidase M (CPM) offered the first candidate mechanism. CPM cleaves the C-terminal arginine of C5a to give C5a-des-Arg (29). There are two problems with this scenario. First, CPM is only macrophage-specific in humans; mouse cells like BMDMs do not appear to express it. Second, CPM trimming of C5a does not fully inactivate it, but reduces both its receptor affinity and efficacy (43). It is not clear whether this would of itself support a self-generated gradient. In any case, mass spectrometry of the cell supernatant exposed to cells revealed no evidence of C5a-des-Arg in mouse BMDMs. The second mechanism is through clathrin-mediated endocytosis (44), where cells take in the chemoattractant ligand attached to its surface G-protein coupled receptor (GPCR) by endocytosing the receptor-ligand complex and targeting it to lysosomes. Our confocal experiments and their analysis indicate that BMDMs use clathrin mediated endocytosis for C5a uptake (Figure 4).

Self-generated chemotaxis has an interesting and complex relationship with the initial concentration of the attractant. In simple SGGs the number of cells performing chemotaxis to the

chemoattractant increases with the concentration of chemoattractant. There is an ideal attractant concentration. Below this, relatively few cells migrate, and the gradient is not robust. Above it, saturation makes the gradient less legible, so cells align less accurately; and it takes an increased time for the chemotaxis to start, because it takes longer for cells to remove enough attractant. This is exactly how macrophages behave in response to homogeneous C5a. We have therefore shown that cells take up C5a, that a gradient is actually formed, and cells behave as expected; it is quite clear that macrophages are fully able to use self-generated chemotaxis to C5a.

The most surprising outcome of this research is that "normal" chemotaxis – macrophages migrating up externally-imposed, relatively steep gradients of C5a – requires the same processes as self-generated chemotaxis to work efficiently. Clearly when cells are given a defined C5a gradient, they alter it and reinforce it to give themselves the clearest stimulus and the most information possible.

In summary, this work shows the importance of self-generated gradients in BMDM chemotaxis to C5a. In the presence of macrophages, C5a gradients are more flexible, and more complex, than was previously thought.

379 **MATERIALS AND METHODS**
380

381 **Cell Culture**

382 The stem cells were extracted from the bone marrow of the wild type mice. The stem cells were
383 supplemented with macrophage differentiation media made of DMEM, 10% heat-inactivated FBS,
384 1% Penicillin-streptomycin, 1% L-glutamine, 50 µM mercaptoethanol and 25ng/ml mouse
385 macrophage colony stimulating factor (mCSF). Fully differentiated macrophages were obtained
386 by day 4. At day 4, the macrophages were rinsed, and fresh macrophage differentiation media was
387 provided. The chemotaxis experiments were performed between 6-8 days. The cells were
388 stimulated with 10ng/ml of LPS experiment a day prior to the chemotaxis experiments.
389

390 **Microscopy**

391 Phase contrast microscopy

392 The time lapse experiments were performed using inverted Nikon ECLIPSE Ti microscope
393 equipped with a LWD 0.52NA condenser, a motorized XY stage, and controlled by commercially
394 available MetaMorph software. The microscope is integrated with an incubator, which enabled us
395 to perform the experiments at 37°C and 5% CO_2. For image acquisition, a 10X 0.3NA air objective
396 was used to capture the images at multiple locations with time interval of 10 minutes.

397 Confocal Microscopy

398 Intensity measurement experiments were performed using Nikon A1R inverted and Zeiss 880
399 confocal microscope equipped with motorized stage. Where appropriate, we used commercially
400 available (Almac Sciences (Scotland) Ltd., Edinburgh) human C5a labelled with AlexaFluor-647®
401 on its N-terminus. Human C5a was used because of the commercial unavailability of fluorescently
402 labelled mouse C5a. Mouse and human C5as share 60% similarity in their amino acid sequence,
403 and mouse macrophages respond and chemotax efficiently to human C5a (45). We have also
404 experimentally verified that BMDM cells chemotax to mouse and human C5a with comparable
405 efficiency.

406 For intensity measurement experiment for SGG experiments shown in Figure 4, 10nM of C5a-
407 AF647® was provided in both inner & outer well of chemotaxis chamber with and without cells.

408 For intensity measurement experiment for imposed gradient shown in Figure 5, 10nM C5a-
409 AF647® was added in the inner well with and without cells in the outer well of the chemotaxis
410 chamber. For all these experiments, the assembled chambers were kept in the incubator at 37°C
411 and 5% CO_2 for 6 hours, followed by the confocal imaging. Image scanning was done with 633nm
412 laser and images were acquired using 40X/1.3NA oil and 60X/1.4NA oil objective. Laser power
413 was adjusted in order to obtain measurable fluorescent signal across the entire bridge. The in-built
414 image stitching feature available in the microscope software was employed to capture the entire
415 bridge. For image analysis, the variation of the fluorescent intensity along the bridge was measured
416 using FIJI/ImageJ (https://imagej.net/software/fiji/).

417 The confocal imaging to evaluate the C5aR1 mediated uptake of C5a AF647® (Figure 6F) were
418 performed using a 60x/1.4NA oil objective on a Nikon NSPARC and Zeiss 980. For analysis,
419 outline was made around all the cells, and their fluorescent intensity was measured. The
420 fluorescent intensity of each cell was subtracted by the average background intensity of the image,
421 followed by measuring the average intensity of all cells in the image.

422 **Statistical Analyses**

423 Statistical analyses were performed using Microsoft Excel (Office 16). All experiments were
424 independently repeated at least three times. Comparisons between groups were evaluated using
425 two-tailed Student's *t*-tests, with significance thresholds designated as $p < 0.05$ (*), $p < 0.001$ (**),
426 and $p < 0.0001$ (***). Data are presented as mean ± standard error of the mean (SEM) unless
427 otherwise indicated, with error bars shown for $n > 3$. For Figure 5E, variability in cell distributions
428 between biological replicates precluded meaningful averaging; therefore, a representative dataset
429 is shown. Although the spatial patterns differed across replicates, the overall conclusions were
430 consistent.

431

432 **Supplementary Materials**

433 **Supplementary Figure S1.** Mass spectrometry report for C5a trimming by cultured human
434 THP-1 macrophages incubated with hC5a. C5a-des-R was seen under all conditions tested.
435 Mouse BMDMs under similar conditions showed no trimming of mC5a.

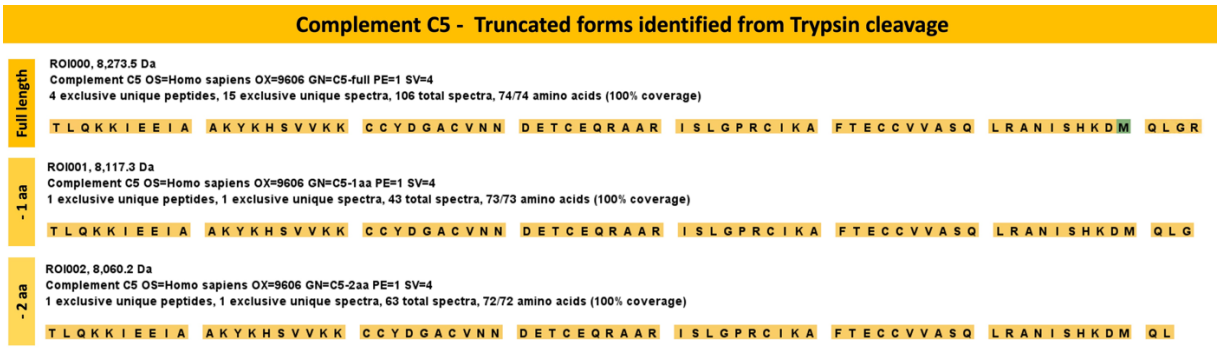

Table S1. Parameters of computational model.

Parameter	Value
Diffusion of C5a	26.5 μm^2/second
Cell diameter	28 µm
Cell speed	1 µm/second
C5a receptor K_d	1 nM
Maximum C5a endocytosis per cell	6.1×10^{-11} nmol/minute

Movie S1. Self-generated C5a gradient. Mouse BMDMs migrating in constant 10nM C5a in an Insall chamber. Top well contains BMDMs plus 10nM C5a. Bottom well contains C5a only. Frame rate 1 frame/10 min.

Movie S2. Computational model. Computational model reproducing the 10nM self-generated gradient shown in Fig. 1A & Movie S1. Parameters as shown in Table S1. Frame rate 1 frame/10 min.

Movie S3. Complex response to different C5a doses. Mouse BMDMs migrating in constant 10nM and 100nM C5a in an Insall chamber. Top well contains BMDMs plus C5a. Bottom well contains C5a only. Frame rate 1 frame/10 min.

Movie S4. Imposed C5a gradient gives similar chemotaxis to self-generated. Mouse BMDMs migrating in an imposed gradient of 0-10nM C5a in an Insall chamber. Top well contains only BMDMs. Bottom well contains 10nM C5a, so a linear gradient is set up between them. Frame rate 1 frame/10 min.

Movie S5. The number of cells in a wave correlates with the amount of C5a. Mouse BMDMs migrating in constant C5a in Insall chambers. Top well contains BMDMs plus the indicated concentration of C5a. Bottom well contains the same concentration of C5a without cells. Frame rate 1 frame/10 min.

Movie S6. Mouse vs. human cells. Mouse BMDMs and cultured human THP-1 cells migrating in constant 10nM C5a in an Insall chamber. Top well contains cells plus 10nM C5a. Bottom well contains C5a only. Frame rate 1 frame/10 min.

Movie S7. Effect of C5aR1 inhibitor PMX-53. Mouse BMDMs migrating in an imposed gradient of 0-10nM C5a in an Insall chamber, with PMX-53 added as indicated. Top well

contains only BMDMs. Bottom well contains 10nM C5a, so a linear gradient is set up between them. Frame rate 1 frame/10 min.

Author contributions

Conceptualization: AK, RHI

Methodology: AK, PT, HD

Investigation: AK, PT, DV, PP, IBF, PS, AS, RD

Visualization: AK, PT, DV

Funding acquisition: RHI, ER, PS

Project administration: AK, RHI

Supervision: RHI, ER, PS

Writing – original draft: AK, RHI

Writing – review & editing: AK, PT, ER, RHI

Competing interests

Authors declare that they have no competing interests.

Data and materials availability:

All data are available in the main text or the supplementary materials.

References

1. Griffith JW, Sokol CL, Luster AD. Chemokines and Chemokine Receptors: Positioning Cells for Host Defense and Immunity. Annual Review of Immunology. 2014;32: 659–702
2. Insall R, Andrew N. Chemotaxis in Dictyostelium: how to walk straight using parallel pathways. Curr Opin Microbiol. 2007;10: 578–581. pmid:18032093
3. Jin T. Gradient sensing during chemotaxis. Curr Opin Cell Biol. 2013;25: 532–537. pmid:23880435
4. Zouwail S, Pettitt TR, Dove SK, Chibalina MV, Powner DJ, Haynes L, et al. Phospholipase D activity is essential for actin localization and actin-based motility in Dictyostelium. Biochem J. 2005;389: 207–214. pmid:15769249
5. Guo R-F, Ward PA. Role of C5a in inflammatory responses. Annu. Rev. Immunol. 2005;23: 821–852
6. He H-Q, Ye RD. The Formyl Peptide Receptors: Diversity of Ligands and Mechanism for Recognition. Molecules. 2017;22: 455. pmid:28335409
7. Thomas MA, Kleist AB, Volkman BF. Decoding the chemotactic signal. J Leukoc Biol. 201829873835
8. David BA, Kubes P. Exploring the complex role of chemokines and chemoattractants in vivo on leukocyte dynamics. Immunol Rev. 2019;289: 9–30. pmid:30977202
9. Heinrich V, Simpson WD, Francis EA. Analytical Prediction of the Spatiotemporal Distribution of Chemoattractants around Their Source: Theory and Application to Complement-Mediated Chemotaxis. Front Immunol. 2017;8: 578. pmid:28603522
10. Hashimoto D, Chow A, Noizat C, Teo P, Beasley MB, Leboeuf M, et al. Tissue-resident macrophages self-maintain locally throughout adult life with minimal contribution from circulating monocytes. Immunity. 2013;38: 792–804. pmid:23601688

11. Varol C, Mildner A, Jung S. Macrophages: development and tissue specialization. Annu Rev Immunol. 2015;33: 643–675. pmid:25861979
12. Gordon S, Plüddemann A. Tissue macrophages: heterogeneity and functions. BMC Biol. 2017;15: 53. pmid:28662662
13. Murphy KM, Weaver C. Janeway's Immunobiology: Tenth International Student Edition with Registration Card. W.W. Norton & Company; 2022.
14. Alanko J, Ucar MC, Canigova N, Stopp J, Schwarz J, Merrin J, et al. Sinking the way: a dual role for CCR7 in collective leukocyte migration. bioRxiv. 20221
15. Insall RH, Paschke P, Tweedy L. Steering yourself by the bootstraps: how cells create their own gradients for chemotaxis. Trends Cell Biol. 2022;32: 585–596. pmid:35351380
16. Tweedy L, Knecht DA, Mackay GM, Insall RH. Self-Generated Chemoattractant Gradients: Attractant Depletion Extends the Range and Robustness of Chemotaxis. PLoS Biol. 2016;14: e1002404. pmid:26981861
17. Zaki M, Andrew N, Insall RH. Entamoeba histolytica cell movement: a central role for self-generated chemokines and chemorepellents. Proc Natl Acad Sci U S A. 2006;103: 18751–18756. pmid:17132728
18. Juin A, Spence HJ, Martin KJ, McGhee E, Neilson M, Cutiongco MFA, et al. N-WASP Control of LPAR1 Trafficking Establishes Response to Self-Generated LPA Gradients to Promote Pancreatic Cancer Cell Metastasis. Dev Cell. 2019;51: 431–445.e7. pmid:31668663
19. Ricklin D, Hajishengallis G, Yang K, Lambris JD. Complement: a key system for immune surveillance and homeostasis. Nat Immunol. 2010;11: 785–797. pmid:20720586
20. Taylor L, Brodermann MH, McCaffary D, Iqbal AJ, Greaves DR. Netrin-1 Reduces Monocyte and Macrophage Chemotaxis towards the Complement Component C5a. PLoS One. 2016;11: e0160685. pmid:27509208

21. Muinonen-Martin AJ, Susanto O, Zhang Q, Smethurst E, Faller WJ, Veltman DM, et al. Melanoma Cells Break Down LPA to Establish Local Gradients That Drive Chemotactic Dispersal. PLoS Biol. 2014;12: e1001966. pmid:25313567
22. Tweedy L, Thomason PA, Paschke PI, Martin K, Machesky LM, Zagnoni M, et al. Seeing around corners: Cells solve mazes and respond at a distance using attractant breakdown. Science. 2020;369: 32855311
23. Tweedy L, Insall RH. Self-Generated Gradients Yield Exceptionally Robust Steering Cues. Front Cell Dev Biol. 2020;8: 133. pmid:32195256
24. Muinonen-Martin AJ, Veltman DM, Kalna G, Insall RH. An improved chamber for direct visualisation of chemotaxis. PLoS One. 2010;5: e15309. pmid:21179457
25. Tweedy L, Susanto O, Insall RH. Self-generated chemotactic gradients-cells steering themselves. Curr Opin Cell Biol. 2016;42: 46–51. pmid:27105308
26. Ma J, Chen T, Mandelin J, Ceponis A, Miller NE, Hukkanen M, et al. Regulation of macrophage activation. Cell Mol Life Sci. 2003;60: 2334–2346. pmid:14625680
27. Susanto O, Koh YWH, Morrice N, Tumanov S, Thomason PA, Nielson M, et al. LPP3 mediates self-generation of chemotactic LPA gradients by melanoma cells. J Cell Sci. 2017;130: 3455–3466. pmid:28871044
28. Donnelly H, Mandrou E, Insall R. Sinking while you swim: A dual role for CCR7 in leukocyte migration. Sci Immunol. 2023;8: eadj3102. pmid:37656778
29. Skidgel RA. Carboxypeptidase M. Handbook of proteolytic enzymes. Elsevier; 2004. pp. 851–854.
30. Solari R, Offord RE, Remy S, Aubry J-P, Wells TNC, Whitehorn E, et al. Receptor-mediated endocytosis of CC-chemokines. Journal of Biological Chemistry. 1997;272: 9617–9620
31. Wu KC, Condon ND, Hill TA, Reid RC, Fairlie DP, Lim J. Ras-Related Protein Rab5a Regulates Complement C5a Receptor Trafficking, Chemotaxis, and Chemokine Secretion in Human Macrophages. J Innate Immun. 2023;15: 468–484. pmid:36882040

32. Aksamit RR, Falk W, Leonard EJ. Chemotaxis by mouse macrophage cell lines. J Immunol. 1981;126: 2194–2199. pmid:7229371
33. Jones GE, Prigmore E, Calvez R, Hogan C, Dunn GA, Hirsch E, et al. Requirement for PI 3-kinase gamma in macrophage migration to MCP-1 and CSF-1. Exp Cell Res. 2003;290: 120–131. pmid:14516793
34. Wells CM, Ridley AJ. Analysis of cell migration using the Dunn chemotaxis chamber and time-lapse microscopy. Cell Migration. 2005
35. Wheeler AP, Wells CM, Smith SD, Vega FM, Henderson RB, Tybulewicz VL, et al. Rac1 and Rac2 regulate macrophage morphology but are not essential for migration. J Cell Sci. 2006;119: 2749–2757. pmid:16772332
36. Kronlage M, Song J, Sorokin L, Isfort K, Schwerdtle T, Leipziger J, et al. Autocrine purinergic receptor signaling is essential for macrophage chemotaxis. Sci Signal. 2010;3: ra55. pmid:20664064
37. van den Bos E, Walbaum S, Horsthemke M, Bachg AC, Hanley PJ. Time-lapse Imaging of Mouse Macrophage Chemotaxis. J Vis Exp. 202032310228
38. Deroy C, Rumianek AN, Wheeler JHR, Nebuloni F, Cook PR, Greaves DR, et al. Assaying Macrophage Chemotaxis Using Fluid-Walled Microfluidics. Advanced Materials Technologies. 2022;7: 5
39. Donnelly H, Kiran A, Insall R. Chemotaxis Assay of Bone Marrow-Derived Macrophages. Methods Mol Biol. 2024;2828: 1–9. pmid:39147965
40. Majumdar R, Sixt M, Parent CA. New paradigms in the establishment and maintenance of gradients during directed cell migration. Curr Opin Cell Biol. 2014;30: 33–40. pmid:24959970
41. Uçar MC, Alsberga Z, Alanko J, Sixt M, Hannezo E. Self-generated chemotaxis of mixed cell populations. bioRxiv. 20240
42. Wong M, Gilmour D. Going your own way: Self-guidance mechanisms in cell migration. Curr Opin Cell Biol. 2021;72: 116–123. pmid:34403875

43. Marder SR, Chenoweth DE, Goldstein IM, Perez HD. Chemotactic responses of human peripheral blood monocytes to the complement-derived peptides C5a and C5a des Arg. J Immunol. 1985;134: 3325–3331. pmid:3884709
44. Mutch LJ, Howden JD, Jenner EPL, Poulter NS, Rappoport JZ. Polarised clathrin-mediated endocytosis of EGFR during chemotactic invasion. Traffic. 2014;15: 648–664. pmid:24921075
45. Chenoweth DE, Goodman MG, Weigle WO. Demonstration of a specific receptor for human C5a anaphylatoxin on murine macrophages. J Exp Med. 1982;156: 68–78. pmid:7086356